

Calibration of Sonographic Gel Probe Covers for In-Vivo Mechanical Testing

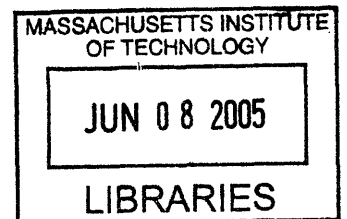
by

Panasaya Charenkavanich

SUBMITTED TO THE DEPARTMENT OF MECHANICAL ENGINEERING IN PARTIAL
FULFILLMENT OF THE REQUIREMENTS FOR THE DEGREE OF

BACHELOR OF SCIENCE IN MECHANICAL ENGINEERING
AT THE
MASSACHUSETTS INSTITUTE OF TECHNOLOGY

JUNE 2005



© 2005 Panasaya Charenkavanich. All rights reserved.

The author hereby grants to MIT permission to reproduce
and to distribute publicly paper and electronic
copies of this thesis document in whole or part.

Signature of Author: _____
Department of Mechanical Engineering
June 6, 2005

Certified by: _____
Simona Socrate
Assistant Professor of Mechanical Engineering
Thesis Supervisor

Accepted by: _____
Ernest G. Cravalho
Professor of Mechanical Engineering
Undergraduate Officer

ARCHIVES
1

Calibration of Sonographic Gel Probe Covers for In-Vivo Mechanical Testing

by

Panasaya Charenkavanich

Submitted to the Department of Mechanical Engineering
on June 6, 2005 in Partial Fulfillment of the
Requirements for the Degree of Bachelor of Science in
Mechanical Engineering

ABSTRACT

Cervical insufficiency is a condition in pregnancy in which the cervix asymptotically dilates in the absence of uterine contractions, resulting in a spontaneous preterm delivery. The condition is often misdiagnosed and presents a significant challenge for the clinical community.

In order to establish better diagnostic criteria for cervical insufficiency and to improve assessment of preterm delivery risk for the individual patient, a non-invasive medical imaging tool, which uses ultrasound elastography to test the mechanical properties of cervical tissue, has been developed. The hand-held ultrasound indentation system will enable in vivo collection of stress-strain data from patients that will provide researchers with the necessary information to be used in material modeling and improve diagnosis of cervical insufficiency.

The device consists of an ultrasound probe, enclosed by a gel-filled cover. The mechanical properties of the covers vary with each cap as well as with time and temperature. Therefore, in order to ensure accurate measurement, the probe covers must be calibrated prior to use.

An experimental study was carried out to examine the effects of various testing conditions on the mechanical behavior of the probe covers. Different freezing and thawing techniques were explored in order to determine favorable conditions in order to preserve the integrity of the probes between the time of manufacture and actual use. From the results of the research, the appropriate combination of testing conditions for probe calibration was determined, as well as freezing and thawing techniques for probe preservation.

Thesis Supervisor: Simona Socrate

Title: Assistant Professor of Mechanical Engineering

Table of Contents

	Page
1.0 Introduction.....	5
Normal Cervical Function.....	5
Cervical Insufficiency.....	5
Causes of Cervical Insufficiency.....	6
Silent Symptoms of Cervical Insufficiency.....	6
Treatment for Cervical Insufficiency.....	6
Current Diagnosis of Cervical Insufficiency.....	7
Ultrasound Elastography.....	7
New Method of Diagnosing Cervical Insufficiency.....	7
Ultrasonic Video Imaging.....	8
2.0 Experimental Materials and Methods.....	9
Probe Mold.....	9
Probe Mock-Ups.....	9
Gel-Filled Probe Covers.....	9
Experimental Apparatus.....	10
Experimental Procedure.....	10
3.0 Theory.....	13
4.0 Results.....	17
5.0 Discussion of Preservation Conditions.....	21
Freezing in Water vs. Air.....	21
Thawing in Water vs. Air.....	21
Water Bath Time.....	23
6.0 Discussion of Testing Conditions.....	25
Varying Test Speed.....	25
Effect of Re-Calibration over Time.....	26
7.0 Conclusion.....	28
References.....	29
Appendix A: Matlab Script for Theoretical Model.....	30

List of Figures

	Page
Figure 1.1	Diagram of female reproductive system..... 5
Figure 1.2	Ultrasound images captured with and without gel-filled probe cover..... 8
Figure 2.1	Gel-filled probe cover..... 10
Figure 2.2	Schematic of experimental set-up..... 10
Figure 2.3	Probe cover during calibration..... 11
Figure 3.1	Compression of thin-walled spherical balloon..... 13
Figure 3.2	Force diagram of compressed balloon..... 15
Figure 3.3	Theoretical force vs. displacement graph..... 16
Figure 4.1	Typical force vs. time graph..... 17
Figure 4.2	Magnification of Figure 4.1..... 17
Figure 4.3	Typical force vs. displacement graph..... 18
Figure 4.4	Maximum and equilibrium forces for fresh probe covers A-J..... 20
Figure 5.1	Force vs. time graph for probe thawed at room temp. for 3 hours..... 21
Figure 5.2	Force vs. displacement graph for probe thawed at room temp. for 3 hours..... 22
Figure 5.3	Force vs. time graph obtained from an oversaturated probe..... 24
Figure 5.4	Force vs. displacement graph obtained from an oversaturated probe..... 24
Figure 6.1	Force vs. time graph for probe tested at 0.1, 0.25, and 0.5 mm/s..... 25
Figure 6.2	Force vs. displacement graph for probe tested at 0.1, 0.25, and 0.5 mm/s..... 26
Figure 6.3	Force vs. time graph after 1, 10, and 30 minutes..... 27
Figure 6.4	Force vs. displacement graph after 1, 10, and 30 minutes..... 27

List of Tables

	Page
Table 4.1	Experimental results for probe covers A-J..... 19
Table 5.1	Weight change in probe covers A-J thawed in water bath..... 23
Table 6.1	Experimental results of different testing speeds..... 25

1.0 Introduction

Normal Cervical Function

The cervix is an organ located at the end of the uterus and at the top of the vagina. It is situated in the female pelvis between the bladder and rectum (see Figure 1.1).

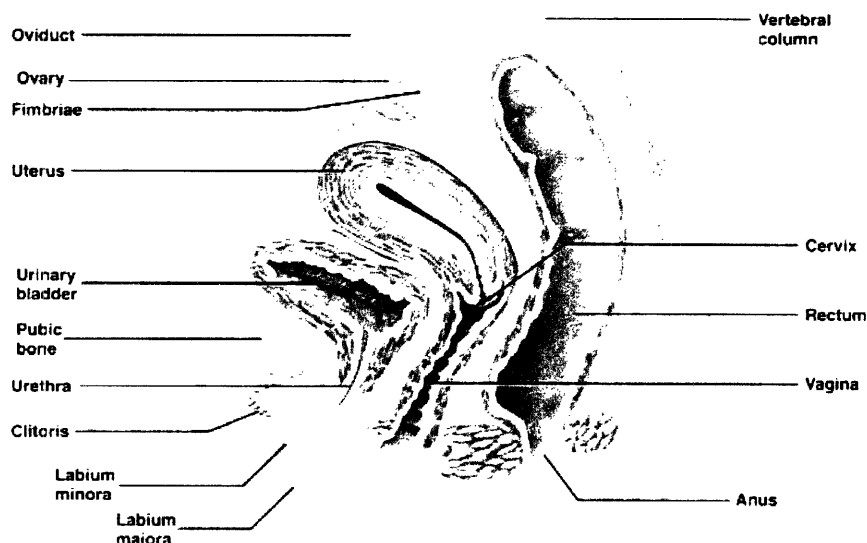


Figure 1.1: Diagram of female reproductive system.¹

The cervical canal passes through the cervix, allowing the menstrual period and fetus to pass from the uterus into the vagina, as well as sperm to pass from the vagina into the uterus. There is a small amount of smooth muscle fibers contained in the cervix, and most of its structure is constituted by dense collagenous tissue. During a normal pregnancy, the cervix is sealed closed with a plug of mucus, holding the fetus in the uterus.²

Cervical Insufficiency

The biomechanical integrity of the cervix is critical in maintaining a healthy pregnancy. Cervical insufficiency represents an extreme case of impaired cervical function in which the cervix dilates without clinically apparent contractions or pain. During dilation, the amniotic membranes bulge through the opening of the cervix and eventually rupture. In many cases, labor is detected once it is too far advanced to stop. Often the baby is unable to survive outside of the uterus at this early stage in the pregnancy. Miscarriages from cervical insufficiency usually occur during the fifth to seventh month of pregnancy. Cervical insufficiency accounts for approximately 20 percent of all pregnancy losses during the second trimester.³ Although its causes are not fully known, cervical insufficiency is believed to be due to either a congenital weakness of the cervix tissue or abnormal anatomy that is hereditary or due to previous trauma.

Causes of Cervical Insufficiency

Risk factors for an insufficient cervix are a history of insufficient cervix with a previous pregnancy; surgery; cervical injury; exposure to DES (diethylstilbestrol), a synthetic estrogen drug given to millions of pregnant women primarily from 1938-1971; as well as anatomic abnormalities of the cervix.^{4,5}

Studies have found that if surgical dilatation of the cervix has been performed on a pelvis, the risk of cervical insufficiency in subsequent pregnancies depends upon the number and degree of dilatation used. Cervical insufficiency is unlikely to occur as a result of a diagnostic dilation and curettage (scraping of the tissue inside the uterus often conducted for irregular periods or after a miscarriage), unless damage to the cervix has occurred. Three or more first trimester surgical terminations of pregnancy have been found to increase risk for cervical insufficiency by approximately 12%.⁴

The taking of biopsies as part of investigating an abnormal Pap smear test does not increase the risk for cervical insufficiency. The more commonly performed Loop diathermy or Large Loop Excision of the Transformation Zone (LLETZ) has not been found to be associated with an increased risk. A less commonly performed procedure called the Cold Knife Cone biopsy, which involves a general anesthesia and removal of a wedge of the cervix to treat cervical pre-cancer, is associated with about a 2% risk increase.⁴

Decreased cervical length, as determined by transvaginal ultrasound, is also associated with an increased risk of preterm delivery.⁴

Silent Symptoms of Cervical Insufficiency

Women with insufficient cervixes typically have “silent” cervical dilation of 2 cm with minimal uterine contractions between 16 - 28 weeks of pregnancy. Once the cervix has dilated to 4 cm, active uterine contractions and membrane rupturing may occur. Some women may experience subtle symptoms prior to miscarriage, such as backaches or heavy vaginal discharge, but there is often little or no bleeding or pain prior to miscarriage.³

Treatment for Cervical Insufficiency

The current treatment for cervical insufficiency is a cervical cerclage, which involves placing a stitch high up around the cervix to help keep it closed. The stitch is placed via either the vagina or an abdominal incision.³ Cerclages are usually performed after the twelfth week of pregnancy, the time after which a woman is least likely to miscarry for other reasons. Vaginal cerclages are removed around 37 weeks of pregnancy in order to allow for a vaginal birth. If the cervix is indeed insufficient as diagnosed, labor will occur fairly rapidly after the stitch is removed. An abdominal cerclage is typically used after a vaginal cerclage has failed. The abdominal cerclage requires an elective caesarean section, and the stitch is usually left in place for future pregnancies. In one study, a reduction in premature delivery rate of 1 in every 25 women was found for those who had a cerclage procedure.⁴

Complications of cerclage include rupture of the membranes at the time of placement and increased risk of infection. For this reason, the procedure is not performed if there are signs of membrane rupture or infection already present.⁴

Current Diagnosis of Cervical Insufficiency

Transvaginal ultrasound has been used to predict cervical insufficiency by measuring cervix length. Typical cervix length is approximately 4 cm as measured on the transvaginal ultrasound. Women with a cervical length of less than 2.5 cm have been found to have a 50% risk of preterm delivery.⁴ Although present methods of diagnosis are promising, currently, the best predictor of cervical insufficiency is a previous pregnancy loss.

Ultrasound Elastography

Ultrasound elastography is a new technique that provides soft-tissue strain images based on the measurements of local tissue deformation in-vivo. Elastography research is advancing at a rapid pace, and the use of the technique is currently being explored in areas of cardiology, urology, and gastroenterology. Elastography is beginning to be tried in clinical practice as a tool for diagnosing cancer.⁶

In one study, ultrasound elastography was used to acquire in-vivo images of the prostate in order to visualize different tissue elasticities and distinguish benign and cancerous tissue. Researchers were able to correctly classify prostate cancer lesions using this sonographic technique.⁷ In another study, the technique was used in imaging in-vivo breast tissue to determine varying degrees of stiffness, which may be useful in discriminating benign from cancerous masses.⁸

New Method of Diagnosing Cervical Insufficiency

A non-invasive, hand-held medical imaging tool using ultrasound elastography has been developed to test the mechanical properties of cervical tissue. The device is used to compress the cervical tissue by applying a small force to the cervix using the end of a vaginal ultrasound probe that is enclosed in soft, gel-filled cover. Both the probe cover and cervix deform as a result of the compression. Pre and post-compression images are obtained, and deformation in the probe cover and cervix is compared using image processing techniques. Two-dimensional images showing tissue stiffness as a function of position, called elastograms, are derived. The stress-strain data can be used to determine the mechanical properties of the cervix tissue. The tool will provide researchers with the necessary information to be used in material modeling and improve diagnosis of cervical insufficiency.

The mechanical properties of the gel-filled probe covers vary with each cover as well as with time and temperature. Therefore, in order to ensure accurate measurement of cervical material properties, the covers must be calibrated prior to use.

Ultrasonic Video Imaging

The covers have been successfully used in-vivo to capture ultrasonic video images by Dr. Michael House at Tufts-New England Medical Center. Still frames from videos taken with and without the probe cover are shown in Figure 1.2. The probe cover was used on a transvaginal probe of a HDI 5000 machine (Philips Ultrasound).⁹

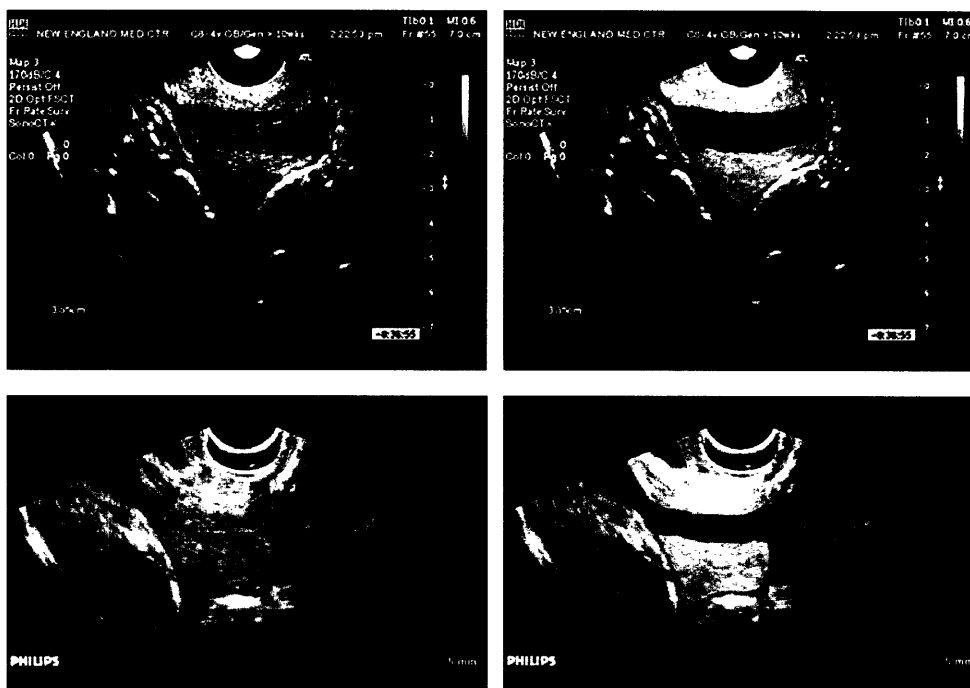


Figure 1.2: Ultrasound images captured with and without gel-filled probe cover.⁹

cervical stroma = yellow

cervical mucosa = red

Top: Saggital, midline view of the cervix at 21-weeks of gestation.

Bottom: Same patient: image taken with the probe cover in place.

2.0 Experimental Materials and Methods

Probe Mold

Prior to casting, the ultrasound probe was covered in a latex sock and coated with mold release spray. The probe was then horizontally submerged halfway in liquid mold-making rubber. Small pins with plastic hemispheres on the end were inserted into the surface of the mold, creating indentations in the mold to help maintain proper alignment during casting. After the mold half had set, it was sprayed with a coating of mold release spray and covered with mold-making rubber until the probe was fully submerged. Once the mold had set, the two mold halves were separated, and the probe was removed.

Probe Mock-Ups

The mold halves were aligned and placed in a plastic container. Smooth-cast liquid plastic compound was poured into the mold and allowed to harden for 10 minutes. The hardened probe was removed from the mold and then polished using fine sandpaper. The probes were then dipped in acrylic polymer emulsion in order to provide a smooth protective coating for the probe.

Gel-Filled Probe Covers

The probe covers were created by combining a urethane top half and a latex/urethane base. To create the top half of the probe cover, the probe mock-ups were dipped in urethane rubber compound and allowed to dry for 24 hours. The dipping procedure was repeated for a total of three layers of urethane. The hardened urethane sock was then rolled off of the probe and cut approximately 1.5 inches from the tip and again at a width of 0.75 inches in order to create the top half of the probe cover and a band, respectively. Air was blown into the probe cover in order to test for leaks.

To create the base half of the probe cover, the probes were dipped in latex rubber and allowed to dry for 24 hours. The probe was then dipped in two layers of urethane, which were allowed to dry between coats. The base sock was trimmed while still on the probe at approximately 3.5 inches from the top of the probe in order to allow for easy removal.

The top half of the probe cover was carefully filled with approximately 6 mL of ultrasound transmission gel. Air bubbles, which could interfere with the ultrasound images, were avoided as much as possible. The top half of the cover was then placed snugly on the cover base. A small elastic band was placed just below the encapsulated ultrasound transmission gel in order to keep the gel from leaking and to keep the two halves together. Urethane was used to seal the joint between the cover halves. Once dry, the small elastic band was removed and the band (previously cut from the probe cover) was placed around the base of the probe tip in order to keep the ultrasound transmission gel from displacing. The final probe cover is shown in Fig. 2.1.

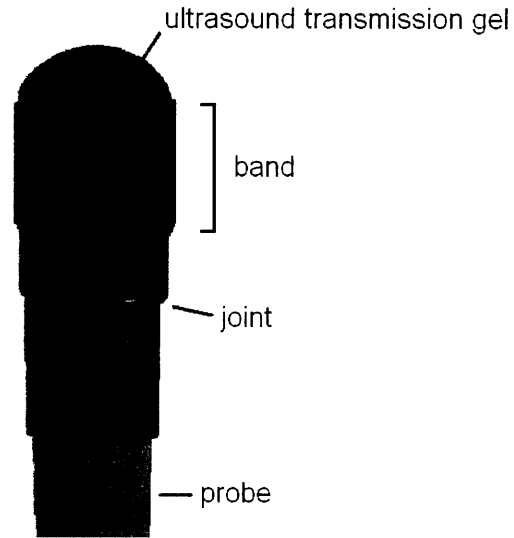


Figure 2.1: Gel-filled probe cover.

Once manufactured, the probe covers were frozen in order to preserve the covers for later use. The proper way to freeze and thaw the covers was explored in order to preserve the integrity of the probes as much as possible.

Experimental Apparatus

A stable Micro Systems' Texture Analyser uniaxial compression test machine was used to gather material data on the probe covers. The apparatus consisted of a movable arm, connected to a 5 kg load cell, which was lowered towards a metal base. The probe was clamped to the movable arm in the upright position. During testing, the arm lowered the probe until contact was made with the metal base. The experimental set-up is shown in a simplified schematic in Figure 2.2.

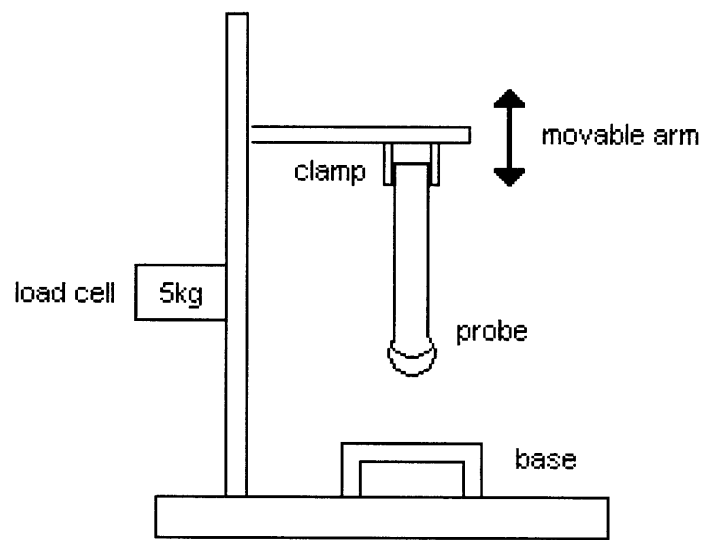


Figure 2.2: Schematic of experimental set-up.

Once the probe made contact with the base, displacement and force readings were measured and recorded in the computer. The program used to gather data was Texture Exponent 32 (TEE32.exe). A photograph of a probe during calibration is shown in Figure 2.3.



Figure 2.3: Probe cover during calibration.

Experimental Procedure

The load cell was first calibrated according to the “Calibrate Force” instructions using a 2 kg weight. The probe was then clamped in the device, and its height was calibrated using the “Calibrate Probe Height” command. The probes were tested at a testing speed of 0.25 mm/s, a trigger force of 0.005 kg, and a displacement of 3 mm.

When a test was triggered, the machine lowered the probe towards the plate. Contact was made between the probe and plate, and the probe was pressed against the plate until a trigger force of 0.005 kg was reached. The probe would then continue to be lowered until displaced by a distance of 3 mm. The probe was held at 3 mm displacement for 15 seconds, and then raised away from the plate. The compression was repeated twice for a hold time of 15 seconds each, and then once for 60 seconds.

The set of three compression tests was performed twice more, with the probe covers being frozen and thawed in between sets. The probes were frozen at a temperature of -17°C and thawed at a temperature of 25°C .

The differences between freezing the probes in air and in water were examined. Two methods of thawing were also explored: thawing in air at room temperature and thawing in a 25°C water bath.

3.0 Theory

The displacement of the gel-filled probe cover during calibration can be modeled as compression of a thin-walled spherical balloon between two plates, depicted in Figure 3.1.

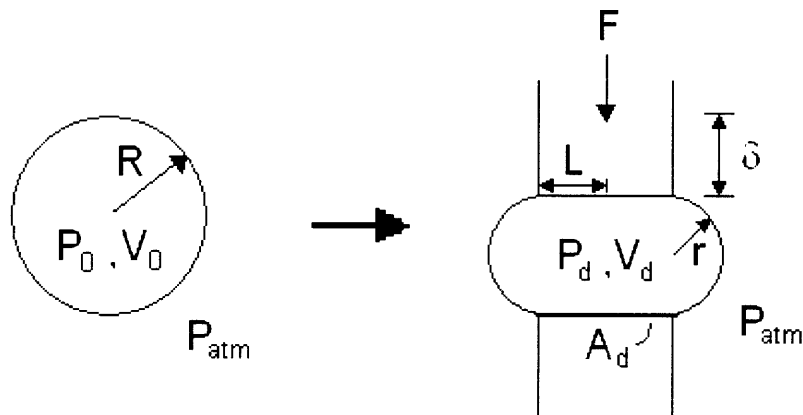


Figure 3.1: Compression of thin-walled spherical balloon.

In Figure 3.1, R is the radius of the uncompressed balloon, P is pressure, V is the volume of the balloon, F is the compression force applied to the balloon, δ is the distance the surface of the balloon is displaced, A_d is the contact area between the probe and metal plate when the balloon is displaced, L is the radius of contact area, and r is the radius of the toroidal (donut-shaped) surface not in contact with the plates during compression.

Pressure is defined as force per unit area. Therefore,

$$F = PA_d = P\pi L^2. \quad (1)$$

As a result of the compression force, the surface of the balloon is displaced by a distance, δ , where:

$$\delta = 2(R-r). \quad (2)$$

The fluid inside the balloon is assumed to be incompressible; therefore, the volume of the balloon is constant:

$$V = V_0 = V_d = \frac{4}{3}\pi R^3, \quad (3)$$

where V_0 is the volume of the uncompressed balloon and V_d is the volume of the displaced balloon. The volume of the displaced balloon is:

$$V_d = V_{cylinder} + V_{toroids} \quad (4)$$

where $V_{cylinder}$ is the volume of the cylindrical core in the center of the compressed balloon and V_{toroid} is the volume of the toroidal region. The volume of the cylindrical core is:

$$V_{cylinder} = (\pi L^2)(2r). \quad (5)$$

The volume of the toroidal region is found using Pappus' Centroid Theorem regarding solids of revolution generated by the revolution of a lamina about an external axis. Applying Pappus' Centroid Theorem to the toroid:

$$V_{toroid} = A_{semicircle} \cdot d = \frac{\pi r^2}{2} \cdot 2\pi(L + \bar{r}), \quad (6)$$

where $A_{semicircle}$ is the area of the semicircular lamina, d is the distance traveled by the centroid of the lamina, and \bar{r} is the geometric centroid of the semicircle.¹⁰ For the semicircular region, the centroid is:

$$\bar{r} = \frac{4r}{3\pi}. \quad (7)$$

Combining Equations 6 and 7, the volume of the toroidal region is:

$$V_{toroid} = \pi^2 r^2 \left(\frac{4r}{3\pi} + L \right). \quad (8)$$

Combining Equations 3, 4, 5 and 8:

$$\frac{4}{3} \pi R^3 = 2\pi L^2 r + \pi^2 r^2 \left(\frac{4r}{3\pi} + L \right). \quad (9)$$

By manipulating Equation 9, the radius of contact area, L , is derived:

$$L = \frac{-3\pi r^2 + \sqrt{3r[3\pi^2 r^3 + 32(R^3 - r^3)]}}{12r}. \quad (10)$$

A force diagram of the compressed balloon is shown in Figure 3.2.

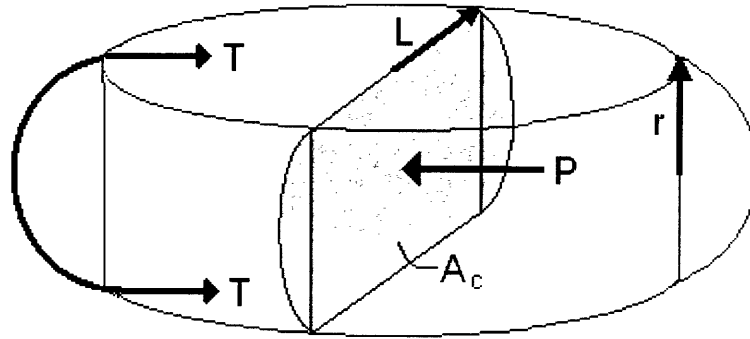


Figure 3.2: Force diagram of compressed balloon.

In Figure 3.2, T is tension in the membrane per unit length, P is pressure in the balloon, and A_c is the cross-sectional area of the displaced balloon. By balancing forces:

$$PA_c = Tp$$

$$P(2L \cdot 2r + \pi r^2) = T(4L + 2\pi r), \quad (11)$$

where p is the perimeter of cross-sectional area. Membrane tension is related to surface area, A_s , by the equation:

$$T = K \frac{\Delta A_s}{A_{s,0}}, \quad (12)$$

where K is the areal modulus of elasticity, ΔA_s is the change in surface area, and $A_{s,0}$ is the surface area of the uncompressed bubble.¹¹ Combining Equations 11 and 12, an expression for pressure is derived:

$$P = K \frac{\Delta A_s}{A_{s,0}} \cdot \frac{4(2L + \pi r)}{r^2(\pi r + 4L)}. \quad (13)$$

The surface area of the uncompressed bubble, $A_{s,0}$, is described by:

$$A_{s,0} = 4\pi R^2, \quad (14)$$

while surface area of the compressed bubble, A_s , is:

$$A_s = 2\pi(L^2 + \pi rL). \quad (15)$$

Combining Equations 11 and 12, the change in surface area, ΔA_s , is:

$$\Delta A_s = 2\pi(L^2 + \pi rL - 2R^2). \quad (16)$$

Combining Equations 1, 2, 13, 14, and 16, an expression for force, F , is determined to be:

$$F = K \frac{2\pi L^2 (2L + \pi r)(L^2 + \pi r L - 2R^2)}{r^2 R^2 (\pi r + 4L)}$$

$$\text{where } r = R - \frac{\delta}{2} \tag{17}$$

$$\text{and } L = \frac{-3\pi r^2 + \sqrt{3r[3\pi^2 r^3 + 32(R^3 - r^3)]}}{12r}.$$

The theoretical graph of force vs. displacement for $K = 0.027 \text{ kg/mm}$ is shown in Figure 3.3.

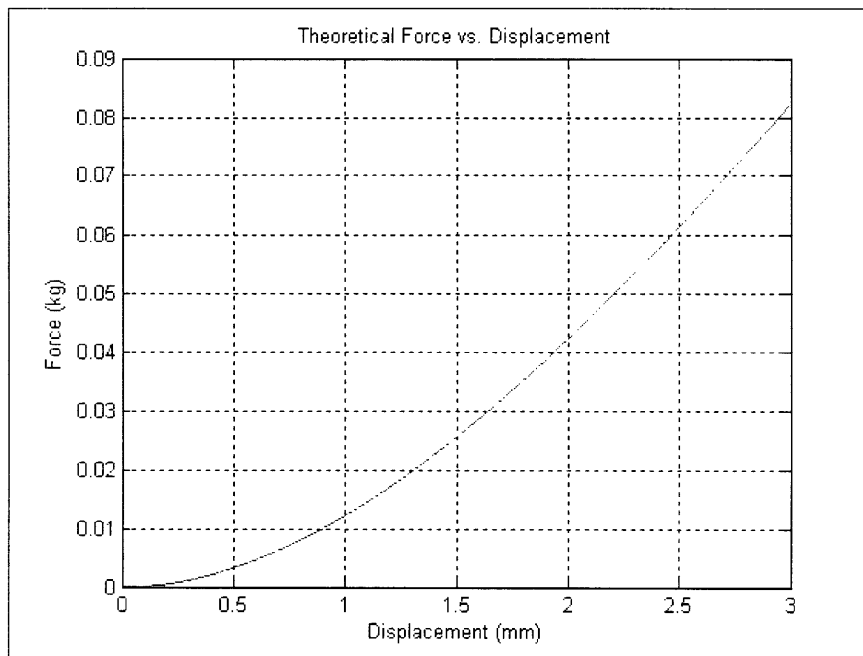


Figure 3.3: Theoretical force vs. displacement graph.

The Matlab program used for the theoretical plot can be found in Appendix A.

4.0 Results

The experimental results of the ten covers tested (probes A-J) produced results similar to the graphs shown in Figures 4.1 - 4.3. The data shows force spiking at F_{max} and then settling to a final equilibrium force, F_{eq} . Initial compression produced forces lower than the following two compressions.

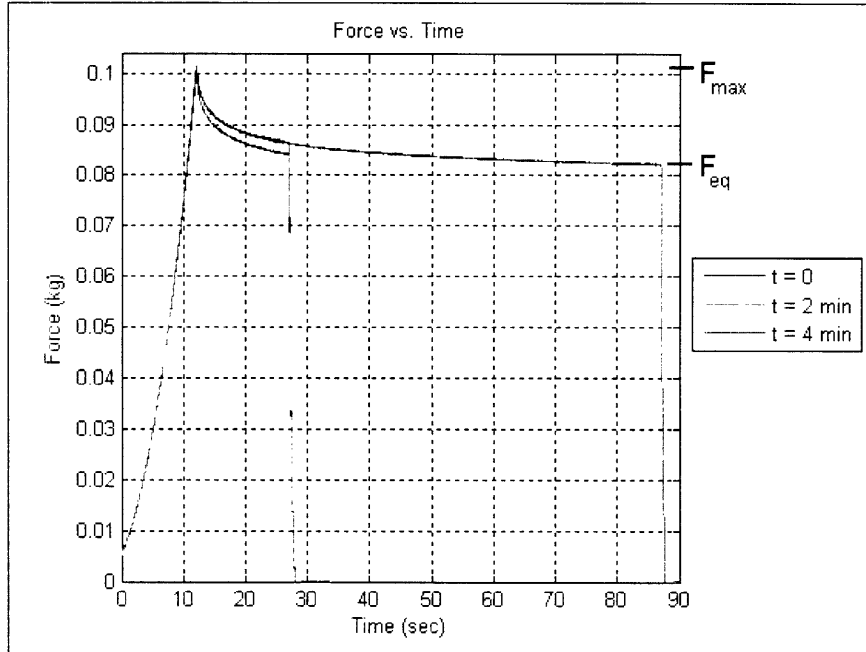


Figure 4.1: Typical force vs. time graph.

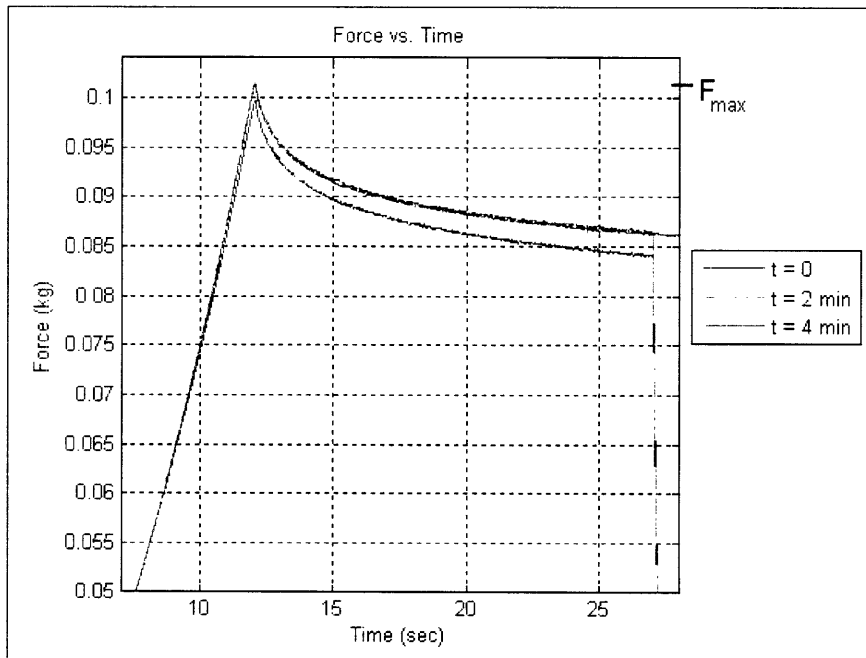


Figure 4.2: Magnification of Figure 4.1.

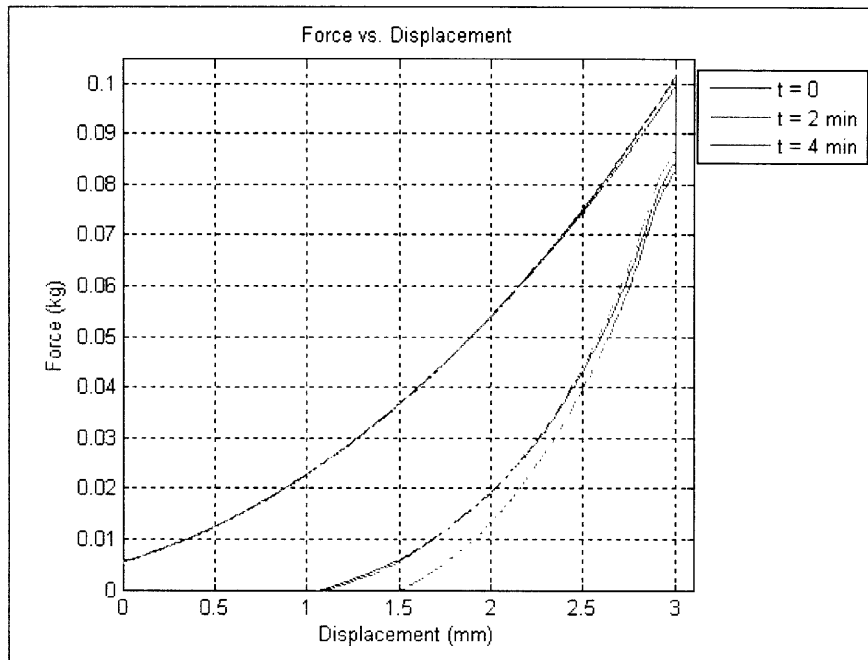


Figure 4.3: Typical force vs. displacement graph.

The data from all 30 trials is shown in Table 4.1 and a bar graph comparing maximum force and steady state force values for all fresh probes is shown in Figure 4.4.

Results indicate that the probe cover behaves as a viscoelastic material. The cover stiffens after initial compression, and then begins to relax. Typically, the second and third compression of the probe cover produced similar responses. This may perhaps be due to the fact that the gel within the probe cover is settled into place during the first compression. The first compression acts a preliminary compression while subsequent compressions produce more accurate data because the gel with in the cover has shifted and settled into its proper testing position.

Table 4.1: Experimental results for probe covers A-J.

Probe	Condition	Weight (g)	Force _{max} (kg)	Force _{eq} (kg)	ΔForce _{eq} (%)
A	fresh	43.68	0.100	0.087	
	after 1 freeze/thaw	42.86	0.086	0.076	12.5
	after 2 freeze/thaw	42.83	0.085	0.074	3.7
B	fresh	39.22	0.076	0.068	
	after 1 freeze/thaw	39.14	0.071	0.062	8.3
	after 2 freeze/thaw	39.12	0.069	0.061	1.8
C	fresh	36.98	0.070	0.063	
	after 1 freeze/thaw	36.88	0.066	0.062	1.1
	after 2 freeze/thaw	36.92	0.064	0.057	7.9
D	fresh	45.21	0.081	0.074	
	after 1 freeze/thaw	45.18	0.075	0.068	7.6
	after 2 freeze/thaw	45.14	0.074	0.068	0.9
E	fresh	41.34	0.099	0.089	
	after 1 freeze/thaw	41.33	0.085	0.076	14.0
	after 2 freeze/thaw	41.31	0.086	0.077	0.7
F	fresh	41.20	0.085	0.075	
	after 1 freeze/thaw	41.20	0.078	0.069	8.3
	after 2 freeze/thaw	41.14	0.078	0.068	1.5
G	fresh	40.92	0.082	0.073	
	after 1 freeze/thaw	40.91	0.075	0.065	10.3
	after 2 freeze/thaw	40.91	0.075	0.066	0.6
H	fresh	37.11	0.070	0.064	
	after 1 freeze/thaw	37.10	0.064	0.056	11.8
	after 2 freeze/thaw	37.05	0.063	0.057	2.0
I	fresh	44.46	0.103	0.093	
	after 1 freeze/thaw	44.47	0.086	0.076	17.9
	after 2 freeze/thaw	44.52	0.089	0.080	4.6
J	fresh	40.94	0.073	0.065	
	after 1 freeze/thaw	41.02	0.072	0.063	3.2
	after 2 freeze/thaw	41.00	0.068	0.060	5.2

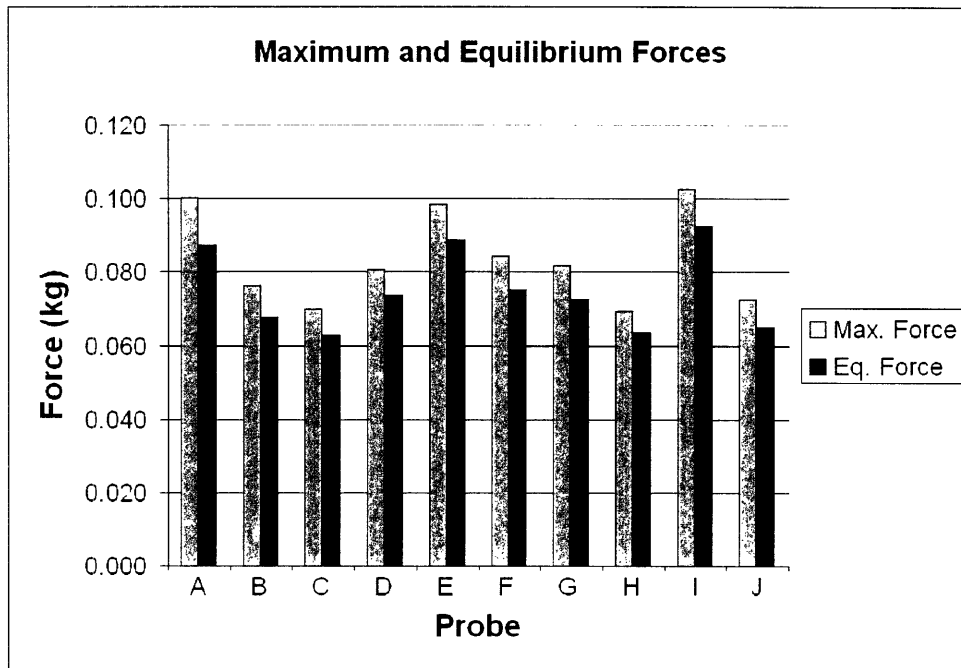


Figure 4.4: Maximum and equilibrium forces for fresh probe covers A-J.

The average maximum force for the fresh probe covers was 0.084 kg, while the average equilibrium force was 0.075 kg.

5.0 Discussion of Preservation Conditions

In real-world use, the probe covers would not be used immediately after assembly. When the probe covers were left at room temperature for several days, the gel-tip caps would continually lose hydration and eventually deflate. Therefore, the appropriate preservation conditions needed to be determined. The probe covers were able to better maintain their integrity when kept frozen. In order to further prolong the life of the covers, the affects of freezing and thawing in both air and water were examined.

Freezing in Water vs. Air

Freezing the probes in water degraded the urethane layers and led to ultrasound gel leakage. The formation of ice around the cover led to corrosion of the urethane and eventual degradation of the urethane seal around the joint between the two probe cover halves.

Freezing the probes in air did affect the mechanical properties of the probes but did not degrade the physical integrity of the probe covers. Therefore, air is a more favorable environment for freezing the probes than water.

Thawing in Water vs. Air

Probes were thawed from a frozen state at room temperature for 3 hours. Although they appeared to be fully thawed, a temperature gradient was present in the probe cover gel. The results from testing these probes, as shown in Figures 5.1 and 5.2, indicate that the gel was not evenly thawed.

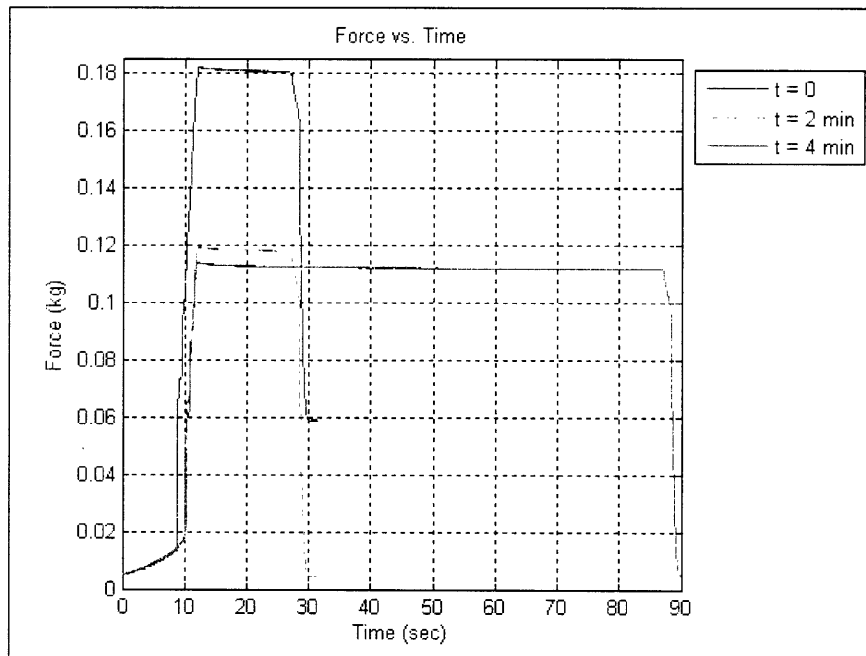


Figure 5.1: Force vs. time graph for probe thawed at room temperature for 3 hours.

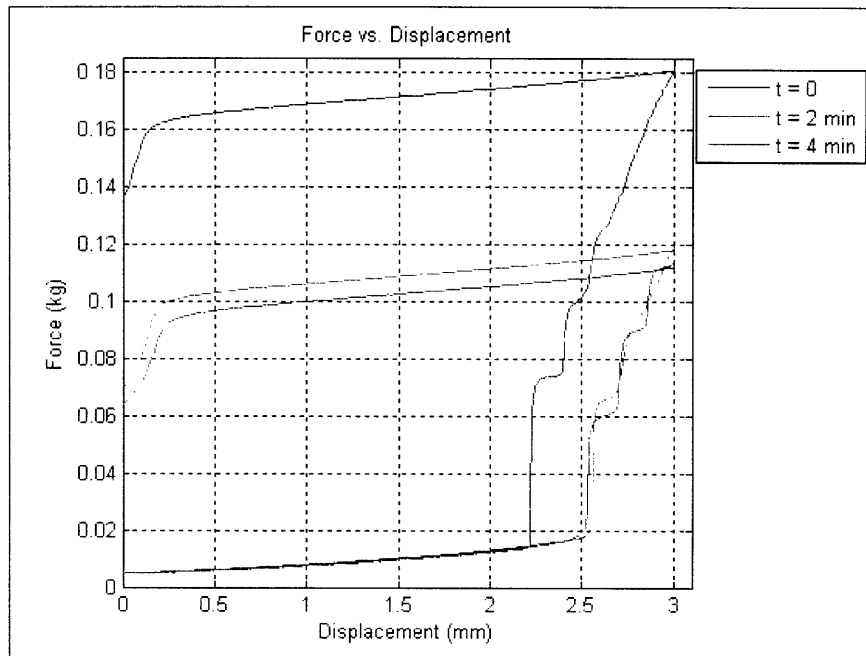


Figure 5.2: Force vs. displacement graph for probe thawed at room temperature for 3 hours.

On the other hand, the probe covers thawed in a water bath produced favorable results similar to fresh probe covers. Weight loss in the probes was minimal. The effect of thawing in a water bath on probe weight is shown in Table 5.1.

Table 5.1: Weight change in probe covers A-J thawed in water bath.

Probe	Condition	Weight (g)	Δ Weight (%)
A	fresh	43.68	
	after 1 freeze/thaw	42.86	1.88
	after 2 freeze/thaw	42.83	0.07
B	fresh	39.22	
	after 1 freeze/thaw	39.14	0.20
	after 2 freeze/thaw	39.12	0.05
C	fresh	36.98	
	after 1 freeze/thaw	36.88	0.27
	after 2 freeze/thaw	36.92	0.11
D	fresh	45.21	
	after 1 freeze/thaw	45.18	0.07
	after 2 freeze/thaw	45.14	0.09
E	fresh	41.34	
	after 1 freeze/thaw	41.33	0.02
	after 2 freeze/thaw	41.31	0.05
F	fresh	41.20	
	after 1 freeze/thaw	41.20	0.00
	after 2 freeze/thaw	41.14	0.15
G	fresh	40.92	
	after 1 freeze/thaw	40.91	0.02
	after 2 freeze/thaw	40.91	0.00
H	fresh	37.11	
	after 1 freeze/thaw	37.10	0.03
	after 2 freeze/thaw	37.05	0.14
I	fresh	44.46	
	after 1 freeze/thaw	44.47	0.02
	after 2 freeze/thaw	44.52	0.11
J	fresh	40.94	
	after 1 freeze/thaw	41.02	0.20
	after 2 freeze/thaw	41.00	0.04

Results show changes in probe weight of no more than 1.88% when thawed in a water bath. One possible reason for the weight retention is that the water in the bath was able to maintain hydration in the probes.

Water Bath Time

When the probe covers were kept in a water bath for a period of 2.5 hours, the covers were over-hydrated and weighed more than before freezing/thawing. The saturation produced a non-homogenous consistency in the cover. The results from these probes are shown in Figures 5.3 and 5.4.

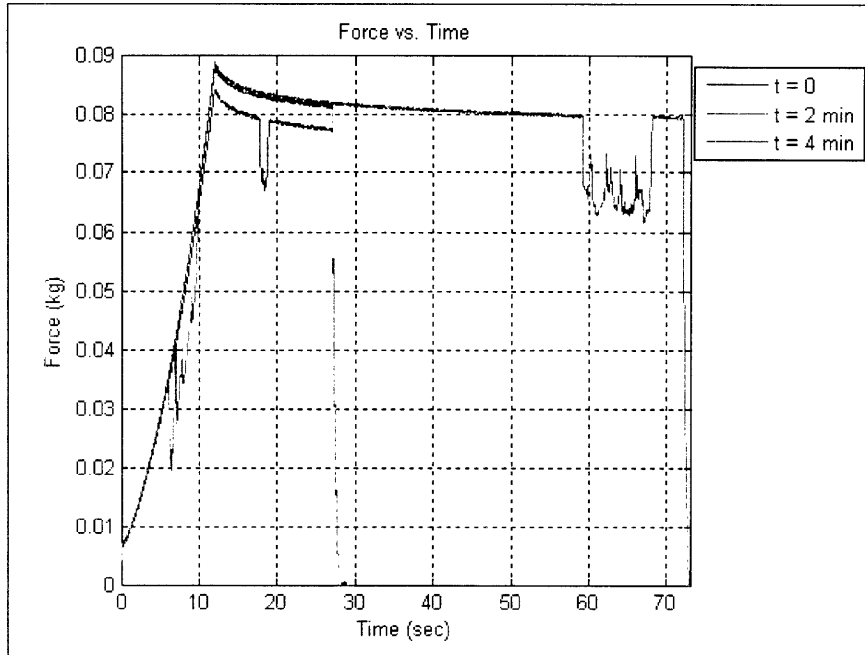


Figure 5.3: Force vs. time graph obtained from an oversaturated probe with weight gain of 0.11%.

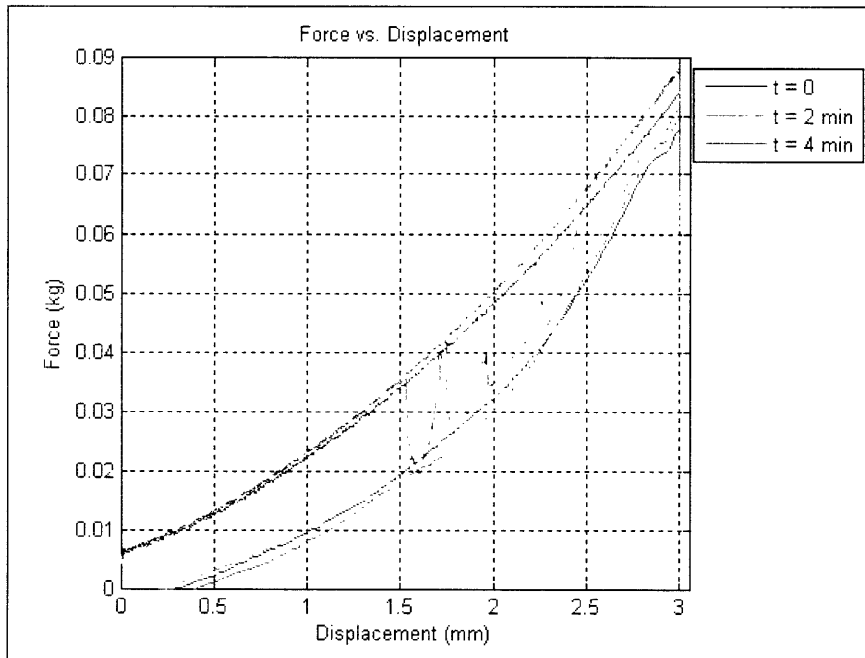


Figure 5.4: Force vs. displacement graph obtained from an oversaturated probe with weight gain of 0.11%.

The random dips and increases in the graphs could perhaps be due to water pockets. Therefore, in order to avoid oversaturation, the probes should be thawed in the water bath for no longer than 1.5 hours.

6.0 Discussion of Testing Conditions

Varying Test Speed

The data obtained when testing a probe at different speeds of 0.10, 0.25, and 0.50mm/s is shown in Table 6.1. Figures 6.1 and 6.2 show the graphical results obtained at the various testing speeds.

Table 6.1: Experimental results of different testing speeds.

Testing Speed (mm/s)	Max. Force (kg)	S.S. Force (kg)
0.10	0.101	0.094
0.25	0.103	0.093
0.50	0.104	0.092

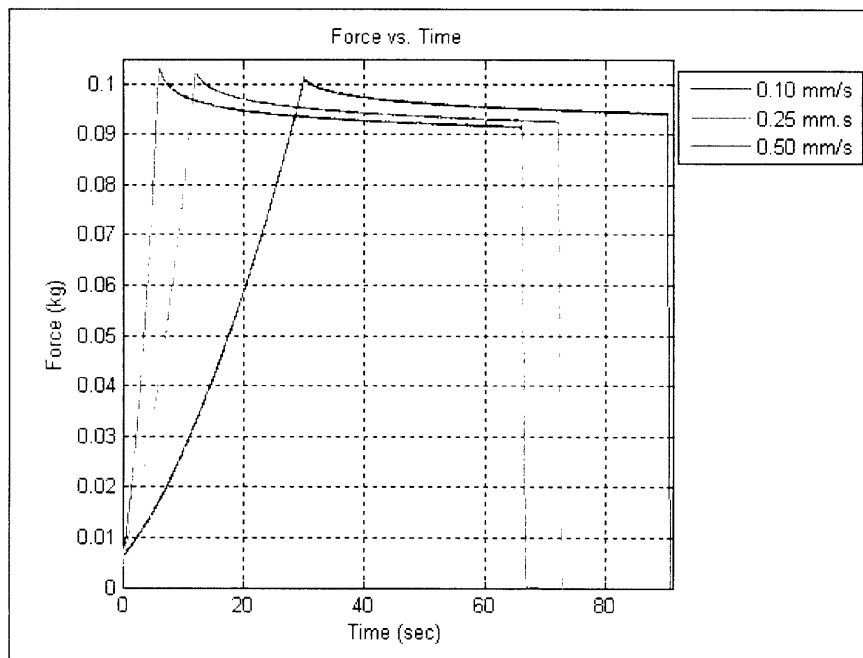


Figure 6.1: Force vs. time graph for probe tested at 0.10, 0.25, and 0.50 mm/s.

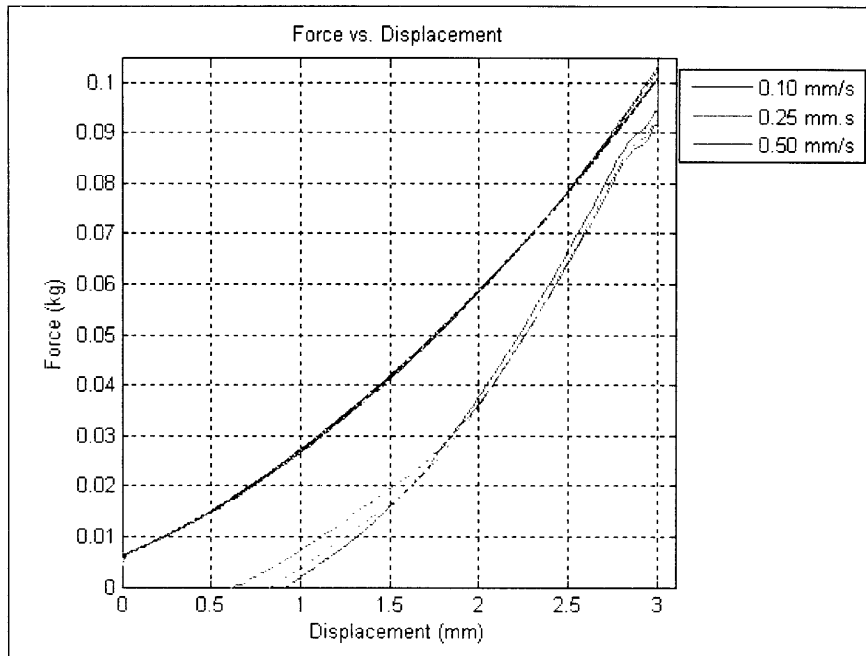


Figure 6.2: Force vs. displacement graph for probe tested at 0.10, 0.25, and 0.50 mm/s.

The results from varying test speed show that the covers are not sensitive to strain rate. Therefore, calibration of the probe covers is not greatly affected by the testing speed.

Effect of Re-Calibration over Time

The compression data taken at 0, 1, 10, and 30 minutes produces a pattern similar to the data taken at 0, 2, and 4 minutes. The graphs in Figures 6.3 and 6.4 show the variance in results when a probe cover is calibrated over a longer period of time.

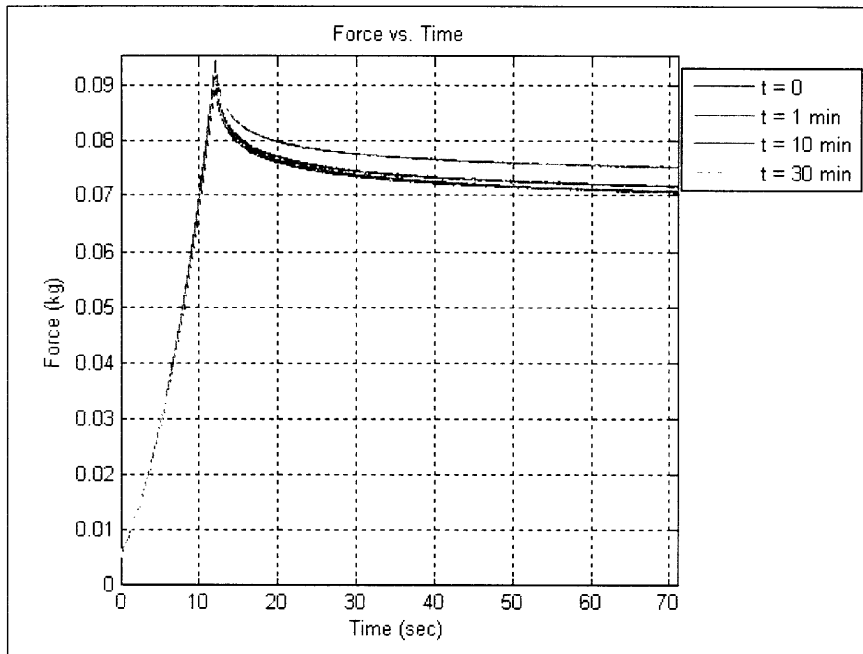


Figure 6.3: Force vs. time graph after 1, 10, and 30 minutes.

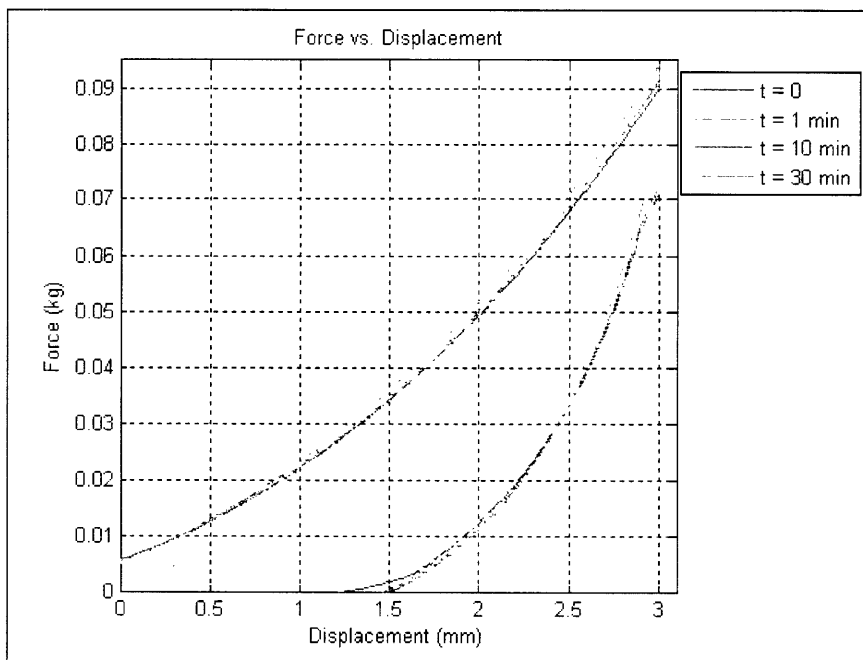


Figure 6.4: Force vs. displacement graph after 1, 10, and 30 minutes.

These graphs produce a similar pattern of distribution to the graphs obtained over a shorter time interval. Therefore, it appears that the behavior of the probe is more dependent on the number of compressions and not the amount of time that has passed between compressions.

7.0 Conclusion

The probe cover behaves as a viscoelastic material that is dependent on the number of times it is compressed. The first compression acts as a preliminary compression to shift the gel of the cover into place, while subsequent compressions produce more accurate data because the gel has settled into its proper testing position. The average maximum force for the fresh probes was 0.084 kg while the average equilibrium force was 0.075 kg.

The probe covers should be stored in a freezer in order to help preserve their integrity. The covers should be thawed in a 25°C water bath for no longer than 1.5 hours, in order to avoid over-hydration. This method of storing the probe covers resulted in preservation of probe hydration and weight, with a decrease in weight of no more than 2%.

References

- [1] Website for Human Physiology and Endocrinology classes at University of Houston. 28 April 2005 <<http://www.uh.edu/~tgill2/image008.jpg>>.
- [2] “Complications.” Essential Baby. 28 April 2005 <<http://www.essentialbaby.com.au/Pregnancy/Complications.cfm>>.
- [3] “Cervical Incompetence.” Health Scout. 10 April 2005 <<http://www.healthscout.com/template.asp?page=ency&ap=68&encyid=361#DefinitionofCervicalInsufficiency>>.
- [4] Tucker, Danny. “Cervical Incompetence.” Women’s Health Information. March 2004. 10 April 2005 <<http://www.womens-health.co.uk/cxinc.asp>>.
- [5] “What is DES?” DES Action USA. 10 April 2005 <<http://www.desaction.org/what.htm>>.
- [6] Han, L., Noble, J.A., Burcher, M. “A novel indentation system for measuring biomechanical properties of in vivo soft tissue.” Ultrasound in Medicine & Biology 29.6 (June 2003): 813-23. <http://www.ncbi.nlm.nih.gov/entrez/query.fcgi?cmd=Retrieve&db=PubMed&list_uids=12837497&dopt=Abstract>.
- [7] Sommerfeld, H. J., Garcia-Schurmann, J.M., Schewe, J., Kuhne, K., Cubick, F., Berges, R. R., Lorenz, A., Pesavento, A., Scheipers, U., Ermert, H., Pannek, J., Philippou, S., Senge, T. “Prostate cancer diagnosis using ultrasound elastography. Introduction of a novel technique and first clinical results.” Der Urologe A 42.7 (July 2003): 941-945. <http://www.ncbi.nlm.nih.gov/entrez/query.fcgi?cmd=Retrieve&db=PubMed&list_uids=12898038&dopt=Abstract>.
- [8] Pellot-Barakat, C., Frouin, F., Insana, M. F., Herment, A. “Ultrasound elastography based on multiscale estimations of regularized displacement fields.” IEEE Transactions on Biomedical Engineering 23.2 (February 2004): 153-63. <http://www.ncbi.nlm.nih.gov/entrez/query.fcgi?cmd=Retrieve&db=PubMed&list_uids=14964561&dopt=Abstract>.
- [9] Paskaleva, Anastassia. “Biomechanics of Cervical Function in Pregnancy: Case of Cervical Insufficiency.” 15 April 2005.
- [10] Weisstein, Eric W. “Pappus's Centroid Theorem.” MathWorld- A Wolfram Web Resource. 5 May 2005 <<http://mathworld.wolfram.com/PappussCentroidTheorem.html>>.
- [11] Fung, Y.C. Biomechanics: Mechanical Properties of Living Tissues. Second Edition. New York: Springer-Verlag New York, 1993. p. 20, 132.

Appendix A: Matlab Script for Theoretical Model

```
% Matlab Script for Theoretical Model

d=[0.0001:0.001:3]';           % d = delta = displacement of probe tip [mm]
R=[5:0.0003:5.89997]';       % R = radius of uncompressed bubble [mm]
K=.07;                         % K = areal modulus of elasticity [kg/mm]

[length, width]=size(d);

for i=1:1:length

r(i)=R(i)-d(i)/2;
L(i)=(-3*pi*r(i)^2+sqrt(3*r(i)*(3*pi^2*r(i)^3-32*(r(i)^3-
R(i)^3))))/(12*r(i));
F(i)=-K*(2*pi*L(i)^2*(2*L(i)+pi*r(i))*(L(i)^2+pi*r(i)*L(i)-
2*R(i)^2))/(r(i)^2*R(i)^2*(pi*r(i)+4*L(i)));

end

plot(d,F)

grid

xlabel('Displacement (mm)')
ylabel('Force (kg)')
title('Theoretical Force vs. Displacement')
```